Revised BCP-D-17-00144

Category: Antibiotics and Chemotherapeutics

Guanine α-carboxy nucleoside phosphonate (G-α-CNP) shows a different inhibitory kinetic profile against the DNA polymerases of human immunodeficiency virus (HIV) and herpes viruses[#]

Jan Balzarini,[a,*] Michael Menni,[b] Kalyan Das,[c] Lizette van Berckelaer,[a] Alan Ford, [d] Nuala M. Maguire,[d] Sandra Liekens,[a] Paul E. Boehmer,[f] Eddy Arnold,[c] Matthias Götte,[b] Anita R. Maguire[d;e]

[a]Rega Institute for Medical Research, KU Leuven, B-3000 Leuven, Belgium

[b]Department of Medical Microbiology and Immunology, University of Alberta, 6-020 Katz Group Centre, Edmonton, AB T6G 2E1, Canada; Department of Biochemistry, McGill University, Montreal, Quebec H3G 1Y6, Canada,

[c]Center for Advanced Biotechnology and Medicine, and Department of Chemistry and Chemical Biology, Rutgers University, Piscataway, New Jersey, USA

[d]Department of Chemistry and [e]School of Pharmacy, Analytical and Biological Chemistry Research Facility, Synthesis and Solid State Pharmaceutical Centre, University College Cork, Ireland

[f]Department of Basic Medical Sciences, The University of Arizona College of Medicine-Phoenix, Phoenix, Arizona, USA

Running title: *G-α-CNP interaction with viral DNA polymerases*

*Corresponding author at: Rega Institute for Medical Research, KU Leuven, Herestraat 49, Box 1030, B-3000 Leuven, Belgium.

E-mail address: jan.balzarini@kuleuven.be (J. Balzarini).

[#]Dedicated to my formal mentor at NIH, Dr. David G. Johns who passed away in December 2016.

ABSTRACT

α-Carboxy nucleoside phosphonates (α-CNPs) are modified nucleotides that represent a novel class of nucleotide-competing reverse transcriptase (RT) inhibitors (NcRTIs). They were designed to act directly against HIV-1 RT without the need for prior activation (phosphorylation). In this respect, they differ from the nucleoside or nucleotide RTIs [N(t)RTIs] that require conversion to their triphosphate forms before being inhibitory to HIV-1 RT. The guanine derivative (G-α-CNP) has now been synthesized and investigated for the first time. The (L)-(+)-enantiomer of G-α-CNP directly and competitively inhibits HIV-1 RT by interacting with the substrate active site of the enzyme. The (D)-(-)-enantiomer proved inactive against HIV-1 RT. In contrast, the (+)- and (-)-enantiomers of G-α-CNP inhibited herpes (i.e. HSV-1, HCMV) DNA polymerases in a non- or uncompetitive manner, strongly indicating interaction of the (L)-(+)- and the (D)-(-)-G-α-CNPs at a location different from the polymerase substrate active site of the herpes enzymes. Such entirely different inhibition profile of viral polymerases is unprecedented for a single antiviral drug molecule. Moreover, within the class of α-CNPs, subtle differences in their sensitivity to mutant HIV-1 RT enzymes were observed depending on the nature of the nucleobase in the α-CNP molecules. The unique properties of the α-CNPs make this class of compounds, including G-α-CNP, direct acting inhibitors of multiple viral DNA polymerases.

Keywords: nucleoside/nucleotide analogs, nucleotide competing RT inhibitor, α-carboxy nucleoside phosphonates, HIV reverse transcriptase, herpes DNA polymerase

Chemical compounds cited in this article

(1*R*,4*S*)-(−)-*cis*-4-acetoxy-2-cyclopenten-1-ol (PubChem CID: 9855498); (1*S*,4*R*)-(+)-*cis*-4-acetoxy-2-cyclopenten-1-ol (PubChem CID: 10154103); Tris (PubChem CID: 6503); EDTA (PubChem CID: 6049); NaCl (PubChem CID: 5234); Formamide (PubChem CID: 713); Bromophenol blue (PubChem CID: 8272); Polyacrylamide (PubChem CID: 6579); Sodium cacodylate(PubChem CID: 2724247); $MgCl_2$ (PubChem CID: 5360315); Dithiothreitol (PubChem CID: 446094); Glutathione (PubChem CID: 124886); KCl (PubChem CID: 4873); Triton X-100 (PubChem CID: 5590); Trichloroacetic acid (PubChem CID: 6421); Sodium pyrophosphate ($Na_4P_2O_7$) (PubChem CID: 24003); $(NH_4)_2SO_4$ (PubChem CID: 22921); Ethanol (PubChem CID: 702); Glycerol (PubChem CID: 753).

1. Introduction

A broad variety of antiviral drugs are clinically approved (for an overview, see ref. 1). The majority of these drugs are nucleoside analogues for which the virus-encoded DNA and RNA polymerases are the prime targets for the inhibition of virus replication. Indeed, a variety of nucleoside analogues efficiently inhibit the herpes DNA polymerases encoded by herpes simplex virus type 1 and type 2 (2), varicella zoster virus (VZV) (2, 3) and human cytomegalovirus (HCMV) (2, 4), the reverse transcriptase of retroviruses such as HIV-1 and HIV-2 (5), the DNA polymerase of hepatitis B virus (6), as well as the RNA polymerases specified by several RNA viruses such as respiratory syncytial virus (7), influenza viruses (8), and also flaviviruses as exemplified by hepatitis C virus (9, 10). Such inhibitors need to be activated (phosphorylated) by virus-encoded kinases or by cellular nucleoside/nucleotide kinases to their 5'-triphosphate derivatives, or in case of the acyclic nucleoside phosphonates to their diphosphate derivatives before these nucleoside/nucleotide analogues can be recognized by the viral DNA or RNA polymerases (1-10). The nucleoside analogues are often incorporated in the growing viral DNA or RNA chain, and function as chain terminators (2, 5). Instead, several non-nucleoside derivatives have also been discovered to act against viral polymerases, either at a non-substrate active site of the enzyme [such as the non-nucleoside RT inhibitor (NNRTI) interaction with HIV-1 RT] (11-13) or at the substrate-active site of the RT enzyme [such as the nucleotide-competing RT inhibitor (NcRTI) (i.e. INDOPY)] (14-16). Such agents differ from a classic nucleoside structure and do not need prior metabolic conversion to exhibit inhibitory activity against their specific polymerase target(s).

Members of the nucleoside analogue class of compounds represent the highest number of clinically approved antiviral drugs (1). However, due to their obligatory dependence on cellular metabolism and often inefficient intracellular conversion to their antivirally-active phosphorylated metabolites, efforts have been devoted to deliver directly and more efficiently the nucleoside/nucleotide drugs intracellularly as their activated (mono)phosphorylated derivatives (17-20). Although this approach proved successful in

several cases, the compounds usually still need to be converted to their eventual triphosphate equivalent before being inhibitory against the viral polymerase.

Recently, we have reported an entirely different approach to design nucleotide analogues (Fig. 1) that are directly inhibitory to viral DNA polymerases without the need of additional metabolic conversions (21, 22). The prototype of these novel nucleotide analogues consists of a nucleobase, connected to an α-carboxy phosphonate moiety through a cyclic cyclopentyl linker entity. Crystallographic, kinetic and biochemical studies have shown that such compounds could directly bind to the substrate-active site of HIV-1 RT without any prior metabolic conversion enabling base pairing and active site Mg^{2+} ion chelation similar to the natural dNTPs (21, 23). It was shown that one oxygen of the carboxylate and two oxygens of the phosphonate part of the α-CNP backbone are involved in Mg^{2+} ion coordination. These three oxygens mimic the three chelating $\alpha-$, $\beta-$, and $\gamma-$phosphate oxygen atoms of a dNTP (21, 23).

Although the thymine-, uracil-, cytosine- and adenine-α-CNPs are potent inhibitors of HIV RT, they are less inhibitory to herpes DNA polymerases (21). However, the guanine α-CNP derivative had not been synthesized and evaluated in previous studies. Given the importance of guanine nucleoside analogues as antiherpes (i.e. acyclovir, ganciclovir) or anti-HIV (i.e. abacavir) agents, we now synthesized the guanine α-CNP (G-α-CNP) and investigated its inhibitory activity against HIV-1 RT and herpes DNA polymerases. The G-α-CNP derivative displayed comparable inhibitory activity against HIV-1 RT and the herpes DNA polymerases as the prototype thymine-α-CNP, but showed differences in its inhibitory activity against mutant HIV-1 reverse transcriptases. Its mechanism of action appears to be significantly different for HIV-1 *versus* the herpes DNA polymerases. This novel compound is of interest as a potential dually-active compound with significant concomitant anti-HIV and anti-herpes virus DNA polymerase activity.

2. Materials and methods

2.1. Compound synthesis and characterization data

G-α-CNP [cis-9-{4-[Carboxy(phosphono)methoxy]cyclopentan-1-yl}guanine]

Racemic G-α-CNP was prepared in nine steps starting from 2-cyclopentenone. The materials were purchased from Acros Organic, Fisher Scientific Ireland Ltd. (Dublin, Ireland). The enantiomers (L)-(+)-G-α-CNP and (D)-(−)-G-α-CNP were prepared in seven steps starting from (1*R*,4*S*)-(−)-*cis*-4-acetoxy-2-cyclopenten-1-ol and (1*S*,4*R*)-(+)-*cis*-4-acetoxy-2-cyclopenten-1-ol, respectively. Full details of the synthesis will be described elsewhere. Characterization data: ^{1}H NMR (400 MHz, D_2O): δ 1.08–2.00 (4H, m), 2.00–2.14 (1H, m), 1H 2.40–2.50 (1H, m), 3.93 (0.5H, d, J = 18.2), 3.99 (0.5H, d, J = 18.3) 4.03–4.10 (1H, m), 4.51-4.62 (1H, m), 8.03 (0.5H, s), 8.04 (0.5H, s); ^{13}C NMR (125 MHz, D_2O): δ 9.4, 30.5, 30.6, 37.8, 38.8, 53.3, 53.5, 80.0, 80.5, 115.8, 138.8, 151.2, 153.4, 158.8, 158.9, 177.6; ^{31}P NMR (162 MHz, D_2O): δ 12.36, 12.48; m/z (ES−) 372.1 $[M-H]^-$; HRMS (ES+) Exact mass calculated for $C_{12}H_{17}N_5O_7P$ $[M+H]^+$ 374.0866; found 374.0861.

2.2. Reverse transcriptase, nucleic acids, and small molecules

HIV-1 reverse transcriptase was expressed and purified as described previously (33).

Oligodeoxynucleotides were synthesized and purchased from Integrated DNA Technologies, Coralville, USA. The following sequences were used as templates: PBS36a, GTAACTAGATATCCCTCAGACCCTTTTAGTCAGAAT; PBS36t, GTAACTAGAAATCCCTCAGACCCTTTTAGTCAGAAT, PBS36c, GTAACTAGAGATCCCTCAGACCCTTTTAGTCAGAAT; PBS36g, GTAACTAGACATCCCTCAGACCCTTTTAGTCAGAAT; PPT57, CGTTGGGAGTGAATTAGCC-CTTCCAGTCCCCCCTTTTCTTTTAAAAAGTGGCTAAGA. Primer sequences used were: PPT-17, GCCACTTTTTAAAAGAAAAGGGGGG; , GAGTGGTATAGTGGAGTGAA; 8a,

TTCTGACTAAAAGGGTCTGAGGGAT; PPT+16, AAAGGGGGGACTGGAAGGGCTAATT. Deoxynucleotides were purchased from Integrated DNA Technologies.

2.3. DNA synthesis

A 3-fold excess of PPT-57 DNA template was heat-annealed to 50 nM 5'-fluorolabeled PPT-17 primer, then incubated with 250 nM of RT in a buffer containing 50 mM Tris-HCl (Sigma, St. Louis, MO), pH 7.8, 50 mM NaCl (Sigma), 0.3 mM EDTA (Sigma), and 0.5 µM of each of dATP, dTTP, dGTP, and dCTP (GE Healthcare, Pittsburgh, PA) (33). The samples were preincubated at 37°C for 5 minutes before starting the reactions. For inhibitor dose-response experiments, each of the four inhibitors was titrated up to 100 µM, and the reaction was initiated with 6 mM $MgCl_2$ and allowed to proceed for 3 minutes. The reaction was stopped with 100% formamide loading dye containing traces of bromophenol blue. Samples were resolved on a 12% denaturing polyacrylamide gel followed by phosphorimaging (Amersham Biosciences, Piscataway, NJ). For the dose-response experiments, pausing sites caused by inhibition were quantified and summed; the % inhibition was calculated as the total amount of inhibited product divided by the amount of full-length product plus inhibition products, multiplied by 100. The product fractions were normalized and plotted against inhibitor concentration using GraphPad Prism software; the normalized data was fitted to a *log[inhibitor] versus response* curve with variable slope to extract IC_{50} values for the inhibition of the RT enzymes by the α-CNP.

2.4. Site-specific footprinting

Chemical footprinting with Fe^{2+} of the template strand was conducted using 50 nM 5'-fluorolabeled DNA template (PPT-57) annealed to 150 nM of the primer (PPT+16). The hybrid was incubated with 750 nM HIV-1 RT in a buffer containing 120 mM sodium cacodylate (pH 7), 20 mM NaCl, and 6 mM $MgCl_2$ in a final volume of 50 µL. Increasing concentrations of G-, T- and A-α-CNP were added to the samples. Samples without inhibitor and without Fe^{2+} treatment were also included. Pre-incubation of complexes at 37°C for

10 minutes was performed prior to the treatment with Fe^{2+}. Treatment with Fe^{2+} was performed as previously described (34).

2.5. Reverse transcriptase assay with homopolymeric template/primers

The HIV-I RT assays were also carried out in the presence of artificial homopolymeric template/primers. Poly(A), dT_{12-18}, dC_{12-18}, poly(I), dA_{12-18} and poly(C), dG_{12-18} were from Pharmacia (Uppsala, Sweden). To prepare the template/primers for the RT experiments, 0.15 mM poly(C) and poly(A) were mixed with an equal volume of 0.0375 mM oligo(dG) and oligo(dT), respectively. The reaction mixture (50 µl) contained 50 mM Tris.HCl (Sigma, Overijse, Belgium) pH 7.8, 5 mM dithiothreitol (Roche, Vilvoorde, Belgium), 300 mM glutathione (Sigma), 500 µM EDTA (Sigma), 150 mM KCl (Sigma), 5 mM $MgCl_2$ (Sigma), 1.25 µg of bovine serum albumin (Sigma), an appropriate concentration of the tritium-labeled substrate [CH_3-^{3}H]dTTP or [^{3}H]dGTP (2 µCi/assay) (Moravek Biochemicals, Brea, CA), a fixed concentration of the template/primer poly(A).oligo(dT) (0.015 mM) or poly(C).oligo(dG) (0.015 mM), 0.06% Triton X-100 (Sigma), 10 µl of α-CNP inhibitor solution (containing various concentrations of the compounds), and 1 µl of the HIV-1 RT preparation. The reaction mixtures were incubated at 37°C for 30 minutes, at which time 100 µl of calf thymus DNA (GE Healthcare, Diegem, Belgium) (150 µg/ml), 2 ml of $Na_4P_20_7$ (Sigma) (0.1 M in 1 M HCl), and 2 ml of trichloroacetic acid (Merck, Darmstadt, Germany) (10% v/v) were added. The solutions were kept on ice for 30 minutes, after which the acid-insoluble material was washed and analyzed for radioactivity. For the experiments in which the 50% inhibitory concentration (IC_{50}) of the test compounds was determined, fixed concentrations of 1.25 µM [^{3}H]dTTP or 2.5 µM [^{3}H]dGTP were used. In the assays in which the IC_{50} and K_i values of the test compounds were determined with respect to the template/primers, appropriate concentrations of template/primer were used. For the experiments in which the K_i values of the test compounds were determined with respect to the template/primers, appropriate concentrations of the template/primers were used in the presence of a fixed concentration of 2.5 µM [^{3}H]dGTP.

2.6. Enzyme assay with HCMV DNA polymerase

The pGEM3Z-CMV UL54 plasmid for expression of the catalytic subunit (UL54 protein) of HCMV DNA polymerase was a generous gift from T. Cihlar (Gilead Sciences, Foster City, CA) (35). Protein expression was performed with the TnT® SP6 Quick Coupled Transcription/Translation System (Promega) (36). The plasmid was added (at 10 ng per µl volume) to the TnT® mix containing 0.5 mM $MgCl_2$ and 10 mM potassium acetate (Janssen Chimica, Beerse, Belgium), and the mixture was incubated for 3 hours at 30°C. To perform the HCMV DNA polymerase assay, 4 µl of the TnT® reaction product was added to a 46 µl mixture to obtain 25 mM Tris.HCl pH 8.0, 100 mM $(NH_4)_2SO_4$ (Sigma), 0.5 mM dithiothreitol, 10 mM $MgCl_2$, 0.2 mg/ml bovine serum albumin, 5 % glycerol (Acros, Geel, Belgium), 150 ng per µl activated calf thymus DNA (from Amersham Biosciences, Piscataway, N.J.), 100 µM of each of the three unlabeled dNTPs (GE Healthcare), and 0.5 µM of the rate-limiting tritium-labeled dNTP, and serial dilutions of the α-CNP. After 60 minutes incubation at 37°C, nucleic acids were precipitated by addition of 1 ml of ice-cold 5% TCA and 20 mM $Na_4P_2O_7$, then spotted onto glass microfiber filters (type G/C; GE Health Care UK Limited, Buckinghamshire, UK) and further washed with 5% TCA and ethanol (BDH Prolabs, Dawsonville, GA) to remove free radiolabeled dNTP. Radioactivity was determined in a Packard (Perkin Elmer, Zaventem, Belgium) Tri-Carb 2300 TR liquid scintillation counter. All radiolabeled materials were obtained from Moravek (Brea, CA).

2.7. Enzyme assay with herpes simplex virus type 1 (HSV-1) DNA polymerase and cellular DNA polymerases α and β

HSV-1 DNA polymerase catalytic subunit (UL30) was expressed in *S. frugiperda* cells and purified as previously described (37). The experiments described here used UL30 fraction V. The reaction mixture (40 µl) for the HSV-1 DNA polymerase and cellular DNA polymerase α and β assays contained 4 µl of Premix (200 mM Tris.HCl pH 7.5; 2 mM DTT; 30 mM $MgCl_2$), 4 µl of BSA (5 mg/ml), 1.6 µl of activated calf thymus DNA (1.0 mg/ml), 0.8 µl of dCTP (5 mM), 0.8 µl of dATP (5 mM), 0.8 µl of dTTP (5 mM), 2 µl of radiolabeled

[^{3}H]dGTP (1 mCi/ml) (3.2 µM), 18 µl of H_2O, and 4 µl of G-α-CNP at different serial concentrations (i.e., 200, 40, 8, 1.6, 0.32 µM). For testing the T-α-CNP analogue, 2 µl [^{3}H]dTTP (1 mCi/ml) and 0.8 µl unlabelled dCTP, dATP, and dGTP (5 mM) were used. The reaction was started by the addition of 4 µl of recombinant HSV-1 DNA polymerase (kindly provided by M.W. Wathen, at that time at Pfizer, Kalamazoo, MI or P.E. Boehmer, Phoenix, AZ) or human cellular DNA polymerase α or β (Chimerix, Milwaukee, WI) (in 20 mM Tris.HCl pH 8.0; 1 mM DTT; 0.1 mM EDTA; 0.2 M NaCl; 40% glycerol), and the reaction mixture was incubated for 60 minutes at 37°C. Then, 1 ml of ice-cold 5% TCA in 0.02 M $Na_4P_2O_7.10\ H_2O$ was added to terminate the polymerization reaction. The consecutive steps (i.e. capture of the acid-insoluble precipitate onto filters, filter washing and scintillation counting) were done as described above.

2.8. Kinetic analysis

The nature of the kinetic interaction of the inhibitors were analysed by the mixed model using a non-linear regression method available in GraphPad. The mixed model uses a general equation including competitive, uncompetitive and noncompetitive inhibition as special cases. The following equations were used: $V_{max(app)} = V_{max}/[1+I/\alpha Ki]$; $K_{m(app)} = K_m.[1+I/K_i]/[1+I/\alpha Ki]$; $Y = V_{max(app)}.X/[K_{m(app)}+X]$, in which X is substrate concentration, Y is enzyme activity, V_{max} is maximum enzyme velocity, K_m = Michaelis-Menten constant, I is inhibitor concentration, K_i = inhibition constant, and α is a constant that determines the kinetic mechanism. When α = 1, kinetics are noncompetitive. When α is very large, the kinetic model approaches a competitive interaction; when α is very small (but greater than zero), the kinetic model approaches an uncompetitive interaction.

3. Results

3.1. G-α-CNP inhibits HIV and herpes DNA polymerases, but not cellular DNA polymerases

The inhibitory activity of G-α-CNP was first evaluated against HIV, herpes (i.e. HSV-1, HCMV) and cellular DNA polymerases α and β as a racemic mixture of (D)-(-) and (L)-(+). The inhibition by NRTI ddGTP, the pyrophosphate analogue PFA, the NNRTI nevirapine, the NcRTI INDOPY-1, and the prototype (L)-(-)-thymine-α-CNP were determined in this study for comparison (Table 1). The (±)G-α-CNP analogue markedly inhibited HIV-1 RT when poly rC.dG and [^{3}H]dGTP were used as the homopolymeric template/primer and dNTP substrate, respectively, but not in the presence of poly rA.dT and [^{3}H]dTTP. This homopolymeric template/primer-dNTP selectivity was in agreement with the earlier findings that the prototype T-α-CNP was only inhibitory to HIV-1 RT in the presence of its corresponding homopolymeric template/primer poly rA.dT-dTTP, but not when any other template/primer-dNTP pair, including poly rC.dG and dGTP, were used (21). These data point to a nucleobase (i.e. guanine)-specific inhibition of dNTP (i.e. dGTP) incorporation into the corresponding homopolymeric template/primer by (±)-G-α-CNP. The (±)G-α-CNP was an equally potent inhibitor of HIV-1 RT as the (±)T-α-CNP derivative [IC_{50}: 0.62 μM and 0.41 μM (21), respectively] (Table 1).

The enantiopure (L)-(+)-G-α-CNP and (D)-(-)-G-α-CNP derivatives have also been synthesized. It was observed before that the (D)-enantiomers of the α-CNPs showed poor, if any, inhibitory activity against HIV-1 RT (21), and thus, the inhibitory potential of the enantiomeric α-CNP mixtures predominantly resided in the (L)-α-CNP enantiomers. A pronounced inhibitory activity of the (L)-(+)-enantiomer of G-α-CNP was indeed demonstrated (IC_{50}: 0.41 μM), whereas the (D)-(-)-G-α-CNP enantiomer was virtually devoid of anti-HIV-1 RT activity (IC_{50}: 335 μM) (Table 1). The (L)-(+)-G-α-CNP derivative was equally inhibitory to HIV-1 RT as 2',3'-dideoxyguanosine-5'-triphosphate (ddGTP), however, at higher efficacy than PFA, nevirapine, and INDOPY-1 in the presence of the poly rC.dG-dGTP template/primer-dNTP system.

In contrast with HIV-1 RT, inhibition of herpes (i.e. HSV-1, HCMV) DNA polymerases by (±)G-α-CNP was independent of the nature of the competing dNTP used (Table 1). Thus, (±)-G-α-CNP inhibited HSV-1 and HCMV DNA polymerases at the same order of magnitude when either dGTP or dTTP were used as the competing radiolabeled substrate (IC_{50}'s ranging between 8 and 32 μM for (±)G-α-CNP and between 4.2 and 29 μM for (L)-(+)-G-α-CNP). It was also striking to notice that for the HSV-1 and HCMV DNA polymerases the degree of inhibition by the (D)-(-)- and (L)-(+)-G-α-CNP enantiomers did not substantially differ. Thus, selective enzyme inhibition by the (D)-(-)-G-α-CNP and/or (L)-(+)-G-α-CNP enantiomer strongly depended of the nature of the enzyme: (L)-(+)-G-α-CNP proved highly selective in the case of HIV-1 RT, whereas discrimination between (D)-(-)- and (L)-(+)-G-α-CNP was much less striking or even non-existing when the herpes HSV-1 and HCMV DNA polymerases were considered. G-α-CNP (as also T-α-CNP) showed marginal, if any, relevant inhibition of the cellular DNA polymerases α and β pointing to its selectivity for viral DNA polymerases, in particular, herpes DNA polymerases and HIV-1 RT.

3.2. Different kinetic properties of G-α-CNP depending the nature of the DNA polymerase

The homopolymeric template/primer-dGTP-dependent specificity of G-α-CNP against HIV-1 RT strongly suggests competitive inhibition with respect to the incoming corresponding dNTP. Therefore, enzyme inhibition kinetics have been investigated for (±)-G-α-CNP. The data were visualized through Lineweaver-Burk reciprocal substrate *versus* velocity plots and analyzed with the mixed model using a non-linear regression method available in Graph Pad (Table 2). (±)-G-α-CNP was indeed found to competitively inhibit dGTP incorporation into the template/primer poly rC.dG (Fig. 2, panel A) (alpha-value in the mixed model being 1.799) and was shown to suppress the DNA polymerization by HIV-1 RT at a strong trend of non-competitive inhibition with regard to the template/primer (Fig. 2, panel B) (alpha-value in the mixed model being 0.147).

The nature of the kinetic interaction of (±)-G-α-CNP for the herpes DNA polymerases of HSV-1 and HCMV was clearly different. Instead of competitive inhibition with respect to the dGTP for HIV-1 RT, a most

likely mode of noncompetitive kinetics was observed for the HSV-1 and HCMV DNA polymerases using calf thymus DNA and [^{3}H]dGTP as the template/primer and radiolabeled dNTP substrate (Fig. 2, panels C & D) (alpha-value in the mixed model being 0.386 and 0.905, respectively) (Table 2). Our kinetic study findings also imply that (±)G-α-CNP interacts with the substrate-active site of HIV-1 RT, but seems to bind to a location different from the substrate-active site in the herpes (i.e. HSV-1, HCMV) DNA polymerases. When kinetic experiments have been performed with the enantiopure (L)-(+)-G-α-CNP (panels A, B & C) and (D)-(-)-G-α-CNP (panels D & E) derivatives, the different kinetic interactions were confirmed between HIV-1 RT (competitive inhibition) on the one hand, and the herpetic DNA polymerases, on the other (non-competitive or uncompetitive inhibition) (Fig. 3). In Table 3, the kinetic parameters obtained from the non-linear regression analysis by GraphPad for the fitting of the different inhibition models are shown.

3.3. The G-α-CNP derivative retards dNTP incorporation and traps the RT in the post-translational state, but does not incorporate into the HIV-1 RT-catalyzed growing DNA chain

HIV-1 RT-catalyzed DNA synthesis was studied in a gel-based assay to gain more insights into the mechanism of drug action. A heteropolymeric DNA was used with a well-defined nucleotide sequence. All four types of α-CNPs containing either adenine, thymine, cytosine, or guanine nucleobase were included for comparison. The experiments showed specific nucleobase-dependent HIV-1 RT inhibition patterns. A dose-dependent inhibition of DNA synthesis was observed at a single nucleotide site before the predicted location on the template at which the α-CNP would interact (compete) with its complementary natural template nucleobase. Thus, the HIV-1 RT-catalyzed nucleotide extension of the template/primer complex by dGTP was dose-dependently retarded in the presence of (±)-G-α-CNP but not A-, T- or C-α-CNP (most right (fifth) lane series, Fig. 4). Likewise, the α-CNPs containing the other nucleobases behaved also selectively depending on the nature of the competing corresponding natural nucleotide (second, third, and fourth lane series, Fig. 4). The IC_{50}'s of HIV-1 RT inhibition in the gel-based assay were calculated to be 3.1 ± 2.0, 3.6 ± 1.8, 2.2 ± 0.40 and 1.8 ± 1.1 μM for the A-, T-, C- and G-α-CNP derivatives, respectively. Our

findings revealed that (±)-G-α-CNP, like the other α-CNPs, are not incorporated into the growing DNA chain, which would have changed the primer migration. Time-course experiments earlier revealed that the inhibition by the α-CNPs was reversible, whereby the shorter reaction products disappeared in function of time, and the full-length end product was eventually reached irrespective the nature of the α-CNP nucleobase present in the drug-containing reaction mixture (21).

The influence of (±)-G-α-CNP on the precise position of HIV-1 RT on the template/primer was verified with Fe^{2+}-mediated footprinting. The template is cut in a site-specific manner upon binding of the Fe^{2+} cation to the RNase H domain of HIV-1 RT (24). This specific hydrolysis event enables discrimination of the inhibitor interaction in a pre- or post-translocation complex. As shown in Fig. 5, increasing concentrations of (±)-G-α-CNP trap the HIV-1 RT enzyme in a post-translocational complex. In this respect, G-α-CNP could trap 50% of the complexed enzyme population in the post-translocational state at a concentration (0.044 ± 0.002 μM) that was 3- to 20-fold lower than A-α-CNP (0.160 ± 0.034 μM) and C-α-CNP (1.4 ± 0.49 μM) (Fig. 5).

3.4. Inhibition of HIV-1 RT by G-α-CNP is influenced by amino acid mutations in the vicinity of the active site

The (±)-G-α-CNP analogue has been analyzed for its sensitivity against a wide variety of mutant HIV-1 RTs, and the fold-resistance values *versus* wild-type RT were compared with those obtained for the corresponding T-, C-, and A-α-CNP analogues as well as for the NcRTI INDOPY-1 (Table 4). Several of the mutations in HIV-1 RT have been chosen among those that were reported to play a role in susceptibility to INDOPY-1 (14, 25), interact with the cyclopentyl ring of T-α-CNP in the crystal structure (i.e. Y115, Q151, and M184) (21), or affect polymerase translocation and fidelity (i.e. F61A, Y115F) (26, 27). The most striking degrees of sensitivity loss for (±)-G-α-CNP were displayed by the F61A mutant RT enzymes (79-fold), followed by RTs containing the M184I/V (8.7- to 19-fold) and the V75I (8.7-fold) mutation (Table 2). Slight sensitization was observed for the K70E/Q (0.7-fold) mutations, but not for the K70R mutation (2.6-fold). Also, the NNRTI-characteristic L100I and Y181C resistance mutations caused a 5.2-fold resistance, but not

the K103N (1.1-fold), V106A (1.6-fold) and E138K (0.9-fold) mutations. The Y115F mutation conferred 2.3-fold resistance against (±)-G-α-CNP. Interestingly, when M184V was combined with Y115F, the resistance level markedly (synergistically) increased (39-fold). The multidrug resistance-associated mutation Q151M afforded a 3.1-fold lower sensitivity to (±)-G-α-CNP than the wild-type enzyme.

When the effects of the HIV-1 RT mutations on the (±)-G-α-CNP's inhibitory potential were compared with their effects on the sensitivities of the mutant enzymes for the corresponding A-, C-, and T-α-CNPs, a number of interesting observations could be made: (i) Depending on the nature of the nucleobase, the sensitivity level against the mutant enzymes sometimes differed quite substantially. For example, the F61A mutation conferred its most pronounced effects on the G and T analogues (79- and 31-fold, respectively), whereas the A and C analogues were much less affected by this mutation (3.9- and 5.2-fold, respectively). Also, the M184I/V mutations showed 8.7- to 19-fold, 11- to 12-fold, or 16- to 36-fold decreased sensitivity for the G-, C- and T-α-CNP analogues, respectively, but only 1.7- to 2.8-fold decreased sensitivity for the A-α-CNP analogue. (ii) Whereas a slight sensitization was observed for the G-analogue against the mutant K70E/Q enzymes (0.7-fold), such sensitization was more pronounced for C-α-CNP (0.2- to 0.3-fold), but was not significantly present for the T-analogue (0.8- to 1.1-fold), whereas the A-analogue was rather endowed with a 3- to 3.7-fold decreased inhibitory potential. Sensitization was also observed for C-α-CNP against the V106A (0.2-fold) and the Q151M (0.4-fold) mutations and to a lesser extent for the A-α-CNP (in both cases 0.8-fold), but absent for the G- and T-analogues (1.1- to 3.1-fold). (iii) When the inhibition spectrum of C-α-CNP was compared with INDOPY-1, a striking similarity could be observed, although the absolute levels of decreased sensitivity/hypersensitivity degree was usually (but not always) less pronounced for INDOPY-1. For example, the sensitization of C-α-CNP inhibition against K70E/Q, V106A and Q151M (0.2- to 0.4-fold) was also observed for INDOPY-1 (0.2- to 0.7-fold), as was also decreased sensitivity to the C-α-CNP (11- to 12-fold) and INDOPY-1 ($\geq$ 6.7-fold) by the mutant M184I/V enzymes. (iv) Whereas the F61A mutation gave consistently the most striking fold-decrease in sensitivity against all α-

CNPs, it hardly affected the inhibitory potential of INDOPY-1 (1.9- to 2.2-fold). (v) Although the G-, A-, C- and T-α-CNPs show nucleobase-specific inhibitory activity against HIV-1 RT irrespective of the nature of the template/primer and competing dNTP (but corresponding to the nucleobase present in the α-CNPs), INDOPY-1 showed only inhibitory activity when competing with pyrimidine nucleotides (dCTP and dTTP), but not purine nucleotides (dGTP or dATP), as also previously reported (14).

Taken all data together, it seems that the decreased inhibition of (±)-G-α-CNP is highest for the mutant RT enzymes that contain changes in amino acids lining the substrate-binding pocket (i.e. V75I, M184I/V) or interact with the template overhang (i.e. F61A). On the other hand, the absolute levels of decreased sensitivity (or hypersensitization) can markedly differ depending the nature of the nucleobase, pointing to subtle differences in the positioning of the α-CNPs in the substrate-active site of HIV-1 RT.

3.5. Modeling of (L)-(+)-G-α-CNP in the substrate-binding site of HIV-1 RT

The G-α-CNP derivative has been modeled in the substrate-binding site pocket of HIV-1 RT. Analogous to T-α-CNP, binding of a G-α-CNP should satisfy the metal chelation, and interactions with a dCMP as the first base overhang. We used the crystal structure of the RT/DNA/T-α-CNP ternary complex (21, 23) to model an RT/DNA/G-α-CNP complex (Fig. 6), in which the metal chelation geometry, and the conformation and interactions of the cyclopentane ring of G-α-CNP were assumed to be very similar to those of T-α-CNP. Analogous to the conformation of α-CNP of the RT-bound T-α-CNP, (L)-(+)-G-α-CNP, but not (D)-(-)-G-α-CNP, binds favorably at the dNTP-binding site. Residue F61 is located at the base of the β3-β4 fingers loop, and its aromatic side chain is positioned between the first and second template overhangs. Additionally, the side chains of F61, I63, and L74 form a hydrophobic cluster, and the cluster appears to have impact on dNTP binding, incorporation, and excision via repositioning of the template overhang. The L74V mutant RT is less fit for nucleotide incorporation and for excision (28, 29). Molecular modeling suggested that L74V might be affecting the positioning of the first template overhang (30).

The crystal structures of HIV-1 RT/DNA/dATP (or dTTP) were compared to assess differences in the mode of binding of a purine vs. pyrimidine nucleobase, but no significant difference was observed between the bound states of dATP vs. dTTP. However, the dynamic steps leading to (i) the binding and (ii) incorporation of a dNTP, and (iii) translocation after the incorporation might be somewhat dependent on specific nucleobase. HIV-1 RTs containing AZT-resistance mutations (or TAM) that efficiently excise AZT (3'-azido-ddT) do not effectively excise AZG (3'-azido-ddG) (31), which may suggest subtle differences in the preferred positioning of the individual dNTPs and their analogs before and after incorporation. We observed significant differences in resistance to A-, T-, G-, and C-α-CNP derivatives by mutant F61A RT (Table 4). F61A mutation might affect the positioning of the template overhang, and the effect may be different on different types of nucleobases to exhibit and explain the diverse impact on α-CNP analogs.

4. Discussion

We recently reported on α-carboxynucleoside phosphonates as a novel class of nucleoside phosphonate derivatives that do not need metabolic activation to efficiently interact with the virus-encoded DNA polymerases (21, 22). Interestingly, crystallographic, biochemical and kinetic studies revealed that these compounds bind like N(t)RTIs in the substrate-binding pocket of HIV-1 RT, compete with dNTPs that contain the same nucleobase as the α-CNP but, in contrast with NRTIs and NtRTIs, are not covalently attached to the primer (21). Whereas these compounds were relatively potent inhibitors of HIV reverse transcriptase (IC_{50}'s in the nanomolar range), they proved clearly less inhibitory to herpes (i.e. HSV-1, VZV, HCMV) DNA polymerases (IC_{50}'s in the micromolar range) (21).

We have now synthesized the corresponding guanine derivative, and demonstrated that it had comparable inhibitory potencies as the prototype T-α-CNP analogue against HIV-1 RT and the HSV-1/HCMV DNA polymerases. Interestingly, whereas G-α-CNP was a competitive inhibitor of HIV-1 RT with respect to the natural dGTP substrate, G-α-CNP showed non- or uncompetitive inhibition with respect to the natural substrate against the HSV-1 and HCMV DNA polymerases. As a result, the lack of competitive kinetics against the herpes DNA polymerases are suggestive for an independent mutually non-exclusive binding of G-α-CNP and the corresponding natural dNTP to the herpes DNA polymerases, and, therefore, G-α-CNP is not expected to interact with the substrate-binding site of the herpes DNA polymerases. Such a distinct kinetic nature of enzyme interaction between HIV-1 *versus* herpes DNA polymerases is unusual and unprecedented for a single drug molecule, reflecting molecular and functional diversity between different enzymes that have similar enzymatic functionalities. Since the crystallographic complex of HIV-1 RT with α-CNPs such as T-α-CNP revealed binding of the compound in the substrate-binding pocket of HIV-1 RT and G-α-CNP could also be modeled into the HIV-1 RT enzyme's active site, it would be very interesting to obtain crystallographic complexes of the α-CNPs (i.e. G-α-CNP) with the herpes DNA polymerase(s) to reveal and define the binding pocket of the α-CNPs in these herpesvirus-encoded enzymes. According to

the nature of the observed kinetics, binding to the polymerase dNTP substrate active-site domain of the herpes DNA polymerase is rather unlikely. It cannot be excluded that the (D)- and (L)-G-α-CNP derivatives are still able to interact with the pyrophosphate binding site of the herpetic DNA polymerases in such a manner that independent binding of dNTP to the substrate active site is still allowed. However, alternatively, the 3',5'-exonuclease domain of the herpes enzymes may also be a potential candidate site for binding of the α-CNPs. In fact, it has been demonstrated that the antiherpes drug acyclovir (as its triphosphate derivative) can bind to the active site of HSV-1 DNA polymerase (competitive to dGTP binding) keeping the 3',5'-exonuclease activity unaffected (32). This means that both polymerase and 3',5'-exonuclease sites can be independently reached by two different drugs in a non-mutually exclusive manner. If such binding would effectively occur for G-α-CNP, the 3',5'-exonuclease binding pocket should be able to harbor both the (D)-(-)- as well as the (L)-(+)-G-α-CNP enantiomer. The identification of the binding pocket of G-α-CNP in the HSV-1 and HCMV DNA polymerases may allow rational design and synthesis of novel and selective classes of herpes DNA polymerase inhibitors.

The mechanistically newest class of HIV RT inhibitors are the nucleotide competing RT inhibitors (NcRTI) represented by the INDOPY-1 prototype compound (14-16). G-α-CNP closely shares most of the kinetic and biochemical properties of the INDOPY derivatives. A number of RT amino acid mutations lining the substrate-binding pocket (i.e. M184I/V; Y115F) that partially compromise INDOPY-1 inhibitory activity (14), also act as compromising RT mutations for G-α-CNP inhibitory activity. However, other mutations such as F61A markedly affect G-α-CNP inhibition, but not INDOPY-1 inhibition. It should, however, be noted that the RT sensitivity spectrum of the α-CNPs highly depended on the nature of the nucleobase, a property that is also the case for NRTIs when the resistance mutation spectrum of NRTIs with different nucleobases (i.e. AZT, ddI, ddC, and carbovir) were compared. Whereas INDOPY's and α-CNPs share many kinetic and biochemical similarities with regard to HIV-1 RT inhibition, inhibition of HIV-1 RT by INDOPY's are independent from Mg^{2+} interactions and are devoid of any anti-herpes DNA polymerase activity. Thus,

although being NcRTIs, the α-CNPs, *in casu* G-α-CNP inhibit also herpes DNA polymerases, qualifying them as novel inhibitors of multiple viral DNA polymerases.

Conflict of interest statement

AM, AF and JB are co-inventors on a patent application concerning the α-CNPs.

Acknowledgments

The research of JB and SL was supported by the KU Leuven (GOA 15/19 TBA). MG is supported by the Canadian Institutes of Health Research (CIHR). EA acknowledges National Institutes of Health for grant R37 AI027690. PEB gratefully acknowledges the support of grant R03 AI119430 from the National Institutes of Health. The authors are grateful to Mrs. Kristien Minner for technical assistance, and Mrs. Christiane Callebaut and Dr. Annelies Stevaert for dedicated editorial help.

Author contributions

JB coordinated the study. JB, MG, EA, KD, AF and ARM designed the study and wrote the paper. MM, KD, LvB, NMM and SL performed the experiments. PEB expressed, purified and provided HSV DNA polymerase. All authors reviewed the results and approved the final version of the manuscript.

References

1. De Clercq, E., and Li, G. (2016) Approved antiviral drugs over the past 50 years. *Clin. Microbiol. Rev.* **29**, 696-747.
2. Topalis, D., Gillemot, S., Snoeck, R., and Andrei, G. (2016) Distribution and effects of amino acid changes in drug-resistant α and β herpesviruses DNA polymerase. *Nucleic Acids Res.*, in press.
3. Andrei, G., and Snoeck, R. (2011) Emerging drugs for varicella-zoster virus infections. *Expert Opin. Emerg. Drugs* **16**, 507-535.
4. Andrei, G., De Clercq, E., and Snoeck, R. (2009) Drug targets in cytomegalovirus infection. *Infect. Disord. Drug Targets* **9**, 201-222.
5. Cihlar, T., and Ray, A.S. (2010) Nucleoside and nucleotide HIV reverse transcriptase inhibitors: 25 years after zidovudine. *Antiviral Res.* **85**, 39-58.
6. Mak, L.Y., Seto, W.K., Lai, C.L., and Yuen, M.F. (2016) DNA polymerase inhibitors for treating hepatitis B: a safety evaluation. *Expert Opin. Drug Saf.* **15**, 383-392.
7. Fearns, R., and Deval, J. (2016) New antiviral approaches for respiratory syncytial virus and other mononegaviruses: Inhibiting the RNA polymerase. *Antiviral Res.* **134**, 63-76.
8. Stevaert, A., and Naesens, L. (2016) The influenza virus polymerase complex: An update on its structure, functions, and significance for antiviral drug design. *Med. Res. Rev.* **36**, 1127-1173.
9. Eltahla, A.A., Luciani, F., White, P.A., Lloyd, A.R., and Bull, R.A. (2015) Inhibitors of the hepatitis C virus polymerase; mode of action and resistance. *Viruses* **7**, 5206-5224.
10. Götte, M., and Feld, J.J. (2016) Direct-acting antiviral agents for hepatitis C: structural and mechanistic insights. *Nat. Rev. Gastroenterol. Hepatol.* **13**, 338-351.
11. De Clercq, E. (2004) Non-nucleoside reverse transcriptase inhibitors (NNRTIs): past, present, and future. *Chem. Biodivers.* **1**, 44-64.

12. Sluis-Cremer, N., and Tachedjian, G. (2008) Mechanisms of inhibition of HIV replication by non-nucleoside reverse transcriptase inhibitors. *Virus Res.* **134**, 147-156.
13. Schauer, G., Leuba, S., and Sluis-Cremer, N. (2013) Biophysical insights into the inhibitory mechanism of non-nucleoside HIV-1 reverse transcriptase inhibitors. *Biomolecules* **3**, 889-904.
14. Jochmans, D., Deval, J., Kesteleyn, B., Van Marck, H., Bettens, E., De Baere, I., Dehertogh, P., Ivens, T., Van Ginderen, M., Van Schoubroeck, B., Ehteshami, M., Wigerinck, P., Götte, M., and Hertogs, K. (2006) Indolopyridones inhibit human immunodeficiency virus reverse transcriptase with a novel mechanism of action. *J. Virol.* **80**, 12283-12292.
15. Maga, G., Radi, M., Gerard, M.A., Botta, M., and Ennifar, E. (2010) HIV-1 RT inhibitors with a novel mechanism of action: NNRTIs that compete with the nucleotide substrate. *Viruses* **2**, 880-899.
16. Ehteshami, M., Nijhuis, M., Bernatchez, J.A., Ablenas, C.J., McCormick, S., de Jong, D., Jochmans, D., and Götte, M. (2013) Formation of a quaternary complex of HIV-1 reverse transcriptase with a nucleotide-competing inhibitor and its ATP enhancer. *J. Biol. Chem.* **288**, 17336-17346.
17. McGuigan, C., and Balzarini, J. (2006) Aryl furano pyrimidines: the most potent and selective anti-VZV agents reported to date. *Antiviral Res.* **71**, 149-153.
18. Meier, C., and Balzarini, J. (2006) Application of the cycloSal-prodrug approach for improving the biological potential of phosphorylated biomolecules. *Antiviral Res.* **71**, 282-292.
19. Ray, A.S., and Hostetler, K.Y. (2011) Application of kinase bypass strategies to nucleoside antivirals. *Antiviral Res.* **92**, 277-291.
20. Gollnest, T., de Oliveira, T.D., Schols, D., Balzarini, J., and Meier, C. (2015) Lipophilic prodrugs of nucleoside triphosphates as biochemical probes and potential antivirals. *Nat. Commun.* **6**, 8716.
21. Balzarini, J., Das, K., Bernatchez, J.A., Martinez, S.E., Ngure, M., Keane, S., Ford, A., Maguire, N., Mullins, N., John, J., Kim, Y., Dehaen, W., Vande Voorde, J., Liekens, S., Naesens, L., Götte, M.,

Maguire, A.R., and Arnold, E. (2015) Alpha-carboxy nucleoside phosphonates as universal nucleoside triphosphate mimics. *Proc. Natl. Acad. Sci. USA* **112**, 3475-3480.

22. Keane, S.J., Ford, A., Mullins, N.D., Maguire, N.M., Legigan, T., Balzarini, J., and Maguire, A.R. (2015) Design and synthesis of α-carboxy nucleoside phosphonate analogues and evaluation as HIV-1 reverse transcriptase-targeting agents. *J. Org. Chem.* **80**, 2479-2493.
23. Das, K., Balzarini, J., Miller, M.T., Maguire, A.R., DeStefano, J.J., and Arnold, E. (2016) Conformational states of HIV-1 reverse transcriptase for nucleotide incorporation vs pyrophosphorolysis-binding of foscarnet. *ACS Chem. Biol*. **11**, 2158-2164.
24. Götte, M., Maier, G., Gross, H.J., and Heumann, H. (1998) Localization of the active site of HIV-1 reverse transcriptase-associated RNase H domain on a DNA template using site-specific generated hydroxyl radicals. *J. Biol. Chem.* **273,** 10139-10146.
25. Ehteshami, M., Scarth, B., Tchesnokov, E.P., Dash, C., Le Grice, S.F., Hallenberger, S., Jochmans, D., and Götte, M. (2008) Mutations M184V and Y115F in HIV-1 reverse transcriptase discriminate against "nucleotide-competing reverse transcriptase inhibitors". *J. Biol .Chem.* **283**, 29904-29911.
26. Scarth, B., McCormick, S., and Götte, M. (2011) Effects of mutations F61A and A62V in the fingers subdomain of HIV-1 reverse transcriptase on the translocational equilibrium. *J. Mol. Biol.* **405**, 349-360.
27. Fisher, T.S., and Prasad, V.R. (2002) Substitutions of Phe61 located in the vicinity of template 5'-overhang influence polymerase fidelity and nucleoside analog sensitivity of HIV-1 reverse transcriptase. *J. Biol. Chem.* **277**, 22345-22352.
28. Deval, J., Navarro, J.M., Selmi, B., Courcambeck, J., Boretto, J., Halfon, P., Garrido-Urbani, S., Sire, J., and Canard, B. (2004) A loss of viral replicative capacity correlates with altered DNA polymerization kinetics by the human immunodeficiency virus reverse transcriptase bearing the K65R and L74V dideoxynucleoside resistance substitutions. *J. Biol. Chem.* **279**, 25489-25496.

29. Götte, M. (2007) Mechanisms of resistance associated with excision of incorporated nucleotide analogue inhibitors of HIV-1 reverse transcriptase. *Curr. Opin. HIV AIDS* **2**, 103-107.

30. Das, K., Bandwar, R.P., White, K.L., Feng, J.Y., Sarafianos, S.G., Tuske, S., Tu, X., Clark, Jr., A.D., Boyer, P.L., Hou, X., Gaffney, B.L., Jones, R.A., Miller, M.D., Hughes, S.H., and Arnold, E. (2009) Structural basis for the role of the K65R mutation in HIV-1 reverse transcriptase polymerization, excision antagonism, and tenofovir resistance. *J. Biol. Chem.* **284**, 35092-35100.

31. Sluis-Cremer, N., Koontz, D., Bassit, L., Hernandez-Santiago, B.I., Detorio, M., Rapp, K.L., Amblard, F., Bondada, L., Grier, J., Coats, S.J., Schinazi, R.F., and Mellors, J.W. (2009) Anti-human immunodeficiency virus activity, cross-resistance, cytotoxicity, and intracellular pharmacology of the 3'-azido-2',3'-dideoxypurine nucleosides. *Antimicrob. Agents Chemother.* **53**, 3715-3719.

32. Vashishtha, A.K., and Kuchta, R.D. (2016) Effects of acyclovir, foscarnet, and ribonucleotides on herpes simplex virus-1 DNA polymerase: Mechanistic insights and a novel mechanism for preventing stable incorporation of ribonucleotides into DNA. *Biochemistry* **55**, 1168-1177.

33. Le Grice, S.F., and Gruninger-Leitch, F. (1990) Rapid purification of homodimer and heterodimer HIV-1 reverse transcriptase by metal chelate affinity chromatography. *Eur. J. Biochem.* **187**, 307-314.

34. Marchand, B, and Götte, M. (2003) Site-specific footprinting reveals differences in the translocation status of HIV-1 reverse transcriptase. Implications for polymerase translocation and drug resistance. *J. Biol. Chem.* **278**, 35362-35372.

35. Cihlar, T., Fuller, M.D., and Cherrington, J.M. (1997) Expression of the catalytic subunit (UL54) and the accessory protein (UL44) of human cytomegalovirus DNA polymerase in a coupled in vitro transcription/translation system. *Protein Expr. Purif.* **11**, 209-218.

36. De Bolle, L., Manichanh, C., Agut, H., De Clercq, E., and Naesens, L. (2004) Human herpesvirus 6 DNA polymerase: enzymatic parameters, sensitivity to ganciclovir and determination of the role of the A961V mutation in HHV-6 ganciclovir resistance. *Antiviral Res.* **64**, 17-25.

37. Boehmer, P.E. (1996) Expression, purification, and characterization of the herpes simplex virus type-1 DNA polymerase. *Methods Enzymol.* **275**, 16-35.

Table 1. Inhibitory activity of G-α-CNP against viral and cellular DNA polymerases

	IC_{50}[a] (μM)							
	HIV-1 RT[b]		HSV-1 DNA pol[c]		HCMV DNA pol[d]		α DNA pol[e]	β DNA pol[f]
	poly rC.dG	poly rA.dT	calf thymus DNA		calf thymus DNA		calf thymus DNA	calf thymus DNA
	[^{3}H]dGTP	[^{3}H]dTTP	[^{3}H]dGTP	[^{3}H]dTTP	[^{3}H]dGTP	[^{3}H]dTTP	[^{3}H]dGTP	[^{3}H]dGTP
(L,D)-(±)G-α-CNP	0.62 ± 0.19	536 ± 0	8 ± 6	32 ± 11	9.4 ± 0.2	16 ± 8	477 ± 83	531 ± 5
(L)-(+)-G-α-CNP	0.43 ± 0.05	396 ± 48	4.2 ± 0.3	24 ± 15	20 ± 9	29 ± 8	121 ± 75	522 ± 19
(D)-(-)-G-α-CNP	335 ±54	≥500	35 ±19	83 ± 29	20 ± 2.4	75 ± 13	>200	195 ± 7
ddGTP	0.41 ± 0.02	>100	4.5 ± 1.2	>100	48 ± 15	>100	73 ± 8	2.2 ± 1.8
PFA	17 ± 2	0.55 ± 0.01	1.6 ± 0.8	3.5 ± 1.7	7.0 ± 0.7	9.4 ± 6.0	56 ± 12	>100
Nevirapine	2.7 ± 0.4	5.6 ± 4.6	>100	>100	>250	>250	>250	>250
INDOPY	>200	0.26 ± 0.07	>100	>100	>100	>100	>100	>100
(L)-(-)-T-α-CNP	>100	0.41 ± 0.10	-	26 ± 20	-	38 ± 11	229 ± 27	>100

[a]50% inhibitory concentration or compound concentration required to inhibit the polymerase-catalyzed DNA synthesis by 50%.
[b]Enzyme reaction in the presence of the homopolymeric poly rC.dG or poly rA.dT, and radiolabeled [^{3}H]dGTP or [^{3}H]dTTP, respectively.
[c-f]Enzyme reaction in the presence of calf thymus DNA and radiolabeled [^{3}H]dGTP or [^{3}H]dTTP.

Table 2. Kinetic inhibition parameters for (D,L)-(-,+)-G-α-CNP

Enzyme	Parameters	Mode of inhibition				Most likely mode of inhibition
		Mixed model enzyme inhibition	Competitive	Non-competitive	Uncompetitive	
HIV-1 RT (varying dGTP)	α[a]	1.799				
	K_i[b]	0.944	0.455	1.30	0.107 (αK_i)[e]	Competitive
	K_m[c]	6.02	4.59	6.64	8.97	
	R^2[d]	0.990	0.975	0.989	0.969	
HIV-1 RT (varying poly rC.dG)	α[a]	0.147				
	K_i[b]	0.832	0.035	0.169	0.1111 (αK_i)[e]	Non-competitive
	K_m[c]	17.3	15.2	14.6	17.9	
	R^2[d]	0.986	0.915	0.979	0.98	
HSV-1 DNA polymerase (varying dGTP)	α[a]	0.386				
	K_i[b]	9.28	0.521	4.17	3.15 (αK_i)[e]	Non-competitive
	K_m[c]	0.101	0.054	0.089	0.1105	
	R^2[d]	0.981	0.854	0.979	0.9787	
HCMV DNA polymerase (varying dGTP)	α[a]	0.904				
	K_i[b]	9.20	2.12	8.59	5.455 (αK_i)[e]	Non-competitive
	K_m[c]	0.717	0.561	0.708	0.816	
	R^2[d]	0.986	0.927	0.986	0.975	

[a]The alpha-value determines the most likely kinetic mechanism: non-competitive inhibition: alpha-value close to 1; competitive inhibition: alpha-value much higher than 1; uncompetitive inhibition: alpha-value much lower than 1.
[b]K_i, inhibition constant.
[c]K_m, Michaelis-Menten constant.
[d]R_2 value represents a parameter for the goodness of the curve fit.
[e]αK_i: inhibition constant being the product of K_i and alpha.

Table 3. Kinetic inhibition parameters for (L)-(+)-G-α-CNP and (D)-(-)-G-α-CNP

Enzyme	Inhibitor	Parameters	Mode of inhibition				Most likely mode of inhibition
			Mixed model enzyme inhibition	Competitive	Non-competitive	Uncompetitive	
HIV-1 RT	(L)-(+)-G- α-CNP[a]	α[b]	3.918				
		K_i[c]	0.506	0.362	0.850	0.312 (αK_i)[f]	Competitive
		K_m[d]	10.5	9.15	13.4	24.1	
		R^2[e]	0.982	0.980	0.979	0.941	
HSV-1 DNA polymerase	(L)-(+)-G- α-CNP[a]	α[b]	1.202				
		K_i[c]	2.21	0.362	2.56	1.98 (αK_i)[f]	Non-competitive
		K_m[d]	0.084	0.063	0.086	0.094	
		R^2[e]	0.974	0.909	0.974	0.967	
HCMV DNA Polymerase	(L)-(+)-G- α-CNP[a]	α[b]	0.802				
		K_i[c]	11.5	2.13	9.81	6.48 (αK_i)[f]	Non-competitive
		K_m[d]	0.676	0.559	0.657	0.736	
		R^2[e]	0.980	0.926	0.980	0.973	
HSV-1 DNA Polymerase	(D)-(-)-G- α-CNP[a]	α[b]	0.002				
		K_i[c]	7,719	1.97	20.8	15.7 (αK_i)[f]	Uncompetitive
		K_m[d]	0.106	0.032	0.077	0.106	
		R^2[e]	0.980	0.777	0.970	0.980	
HCMV DNA Polymerase	(D)-(-)-G- α-CNP[a]	α[b]	0.213				
		K_i[c]	122	16.3	42.8	20.5 (αK_i)[f]	Non-competitive
		K_m[d]	1.78	1.55	1.51	1.87	
		R^2[e]	0.991	0.946	0.985	0.988	

[a]Varying dGTP.

[b]The alpha-value determines the most likely kinetic mechanism: non-competitive inhibition: alpha-value close to 1; competitive inhibition: alpha-value much higher than 1; uncompetitive inhibition: alpha-value much lower than 1.

[c]K_i, inhibition constant.

[d]K_m, Michaelis-Menten constant.

[e]R_2 value represents a parameter for the goodness of the curve fit.

[f]αK_i: inhibition constant being the product of K_i and alpha.

Table 4. Fold-resistance of the α-CNPs against mutant HIV-1 RTs compared to wild-type (control)

Mutation in HIV-1 RT	G-α-CNP Poly rC.dG [^{3}H]dGTP	A-α-CNP Poly rU.dA [^{3}H]dATP	C-α-CNP Poly I.dC [^{3}H]dCTP	T-α-CNP Poly rA.dT [^{3}H]dTTP	INDOPY-1 Poly rI.dC [^{3}H]dCTP	INDOPY-1 Poly rA.dT [^{3}H]dTTP
F61A	79	3.9	5.2	31	1.9	2.2
K65R	2.1	0.8	1.6	1.5	1.3	1.0
K70E	0.7	3.0	0.2	0.8	0.6	1.5
K70Q	0.7	3.7	0.3	1.1	0.7	2.5
K70R	2.6	3.3	2.3	0.9	0.9	0.6
V75I	8.7	7.0	6.0	2.6	0.9	1.0
L100I	5.2	3.0	0.5	1.4	2.8	3.9
K103N	1.1	0.6	1.5	0.6	1.1	0.6
V106A	1.6	0.8	0.2	1.1	0.4	1.0
Y115F	2.3	0.8	1.1	2.4	2.9	2.8
E138K	0.9	0.7	1.5	1.0	1.0	0.7
Q151M	3.1	0.8	0.4	3.1	0.2	1.6
Y181C	5.2	1.8	1.5	0.9	$\geq$ 6.7	1.3
M184I	19	2.8	12	36	$\geq$ 6.7	5.9
M184V	8.7	1.7	11	16	> 6.7	7.1
M184I + E138K	4.2	13	3.5	16	0.6	1.1
M184V + Y115F	39	5.6	4.1	3.2	$\geq$ 6.7	28
M184V + E138K	6.1	2.6	5.0	3.0	1.0	3.8

Figure legends

Fig. 1. Structural formulae of α-CNPs containing different nucleobases.

Fig. 2. Lineweaver-Burk graphic plots for the inhibition of HIV-1 RT (panels A & B), HSV-1 DNA polymerase (panel C) and HCMV DNA polymerase (panel D) by (±)-G-α-CNP. In panels A and B, homopolymeric rC.dG and [^{3}H]GTP were used as the template/primer and radiolabeled dGTP substrate. In panels C and D, calf thymus DNA and [^{3}H]dGTP were used as the template/primer and radiolabeled dGTP substrate.

Fig. 3. Lineweaver-Burk plots for the inhibition of HIV-1 RT (panel A), HSV-1 DNA polymerase (panels B and D), and HCMV DNA polymerase (panels C and E) by enantiopure (L)-(+)-G-α-CNP and (D)-(-)-G-α-CNP. The template/primer and radiolabeled dNTP substrate were similar as those mentioned in the legend to Fig. 2, panels A, C, and D.

Fig. 4. Non-incorporative nucleotide-competing inhibition of α-CNPs.

Inhibition of HIV-1 RT-catalysed DNA synthesis monitored in dose-response experiments in the presence of a fixed dNTP concentration, T50A DNA template/5'-radiolabeled P1 DNA primer, and increasing concentrations of A-, T-, C- and G-α-CNP, respectively (right block). Specific sites of inhibition by each of the four compounds are located a single residue before the inhibitor- and dNTP-binding sites.

Fig. 5. Post-translocation trapping of HIV-1 RT by α-CNPs.

The precise position of HIV-1 RT on its template/primer was analyzed through Fe^{2+}-mediated footprinting. Upon binding of the Fe^{2+} ion to the RNAse H domain, the template is cut in a site-specific manner that

enables the distinction between pre- and post-translocated complexes. Increasing concentrations of A-, C-, and G-α-CNP trap the HIV-1 RT as a post-translocated complex.

Fig. 6. RT/DNA/T-α-CNP-based modeling of (L)-(+)-G-α-CNP in the substrate binding-site of HIV-1 RT. The template overhang has a cytosine base to allow base pairing with G-α-CNP. The metal ion (B) has distorted octahedral coordination involving three oxygens of G-α-CNP and the side chains of catalytic aspartates D110 and D185 and main chain carbonyl of V111 (not shown)

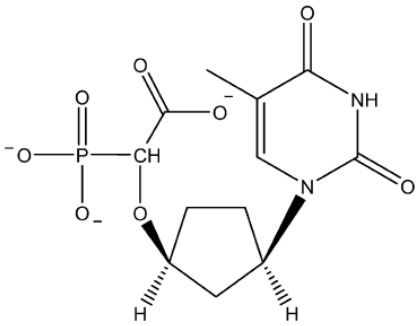

(L)-(−)-T-α-CNP

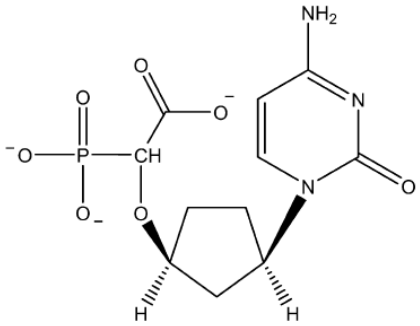

(L)-(−)-C-α-CNP

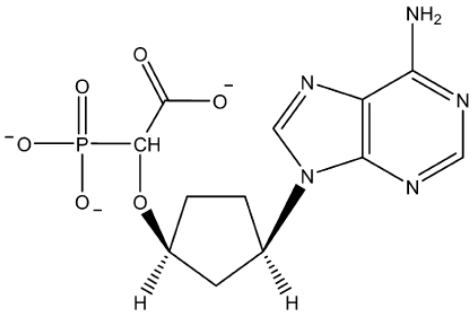

(L)-(−)-A-α-CNP

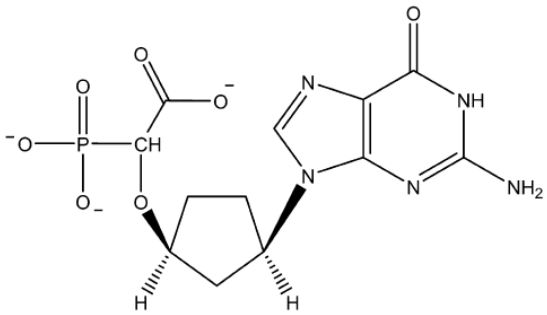

(L)-(+)-G-α-CNP

Fig. 1

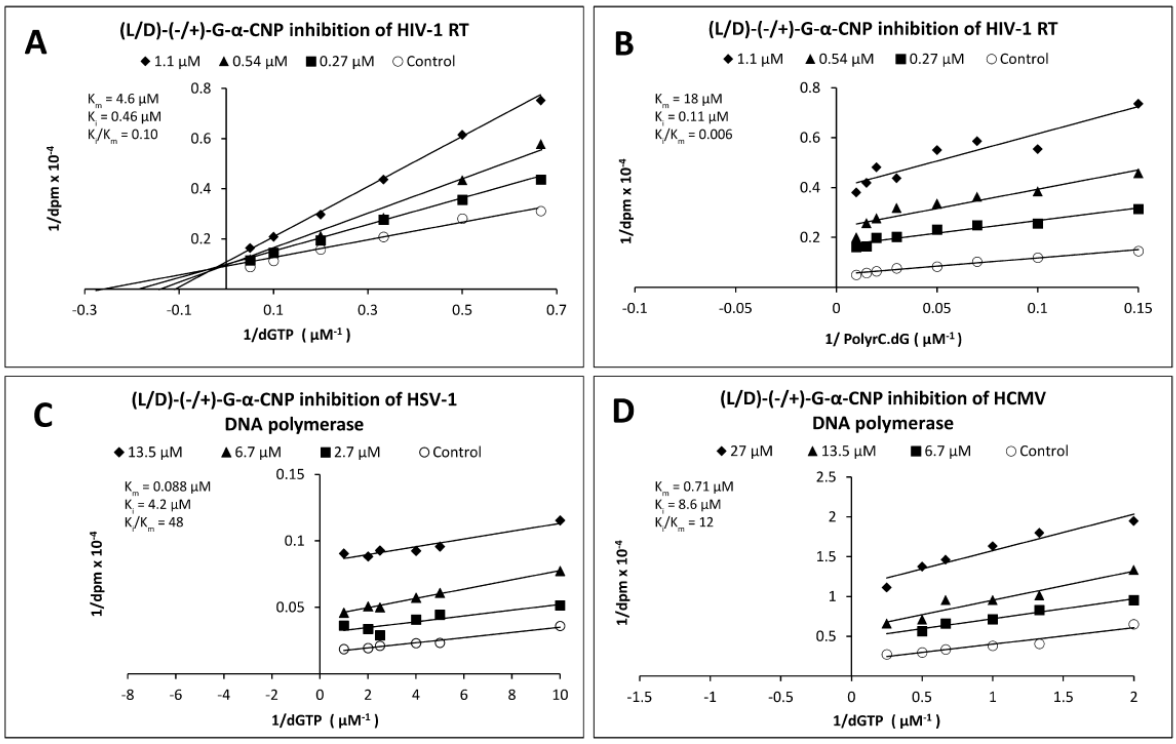
A
(L/D)-(-/+)-G-α-CNP inhibition of HIV-1 RT
◆ 1.1 µM ▲ 0.54 µM ■ 0.27 µM ○ Control
K_m = 4.6 µM
K_i = 0.46 µM
K_i/K_m = 0.10
1/dpm x 10^{-4}
1/dGTP (μM^{-1})
B
(L/D)-(-/+)-G-α-CNP inhibition of HIV-1 RT
◆ 1.1 µM ▲ 0.54 µM ■ 0.27 µM ○ Control
K_m = 18 µM
K_i = 0.11 µM
K_i/K_m = 0.006
1/dpm x 10^{-4}
1/ PolyrC.dG (μM^{-1})
C
(L/D)-(-/+)-G-α-CNP inhibition of HSV-1 DNA polymerase
◆ 13.5 µM ▲ 6.7 µM ■ 2.7 µM ○ Control
K_m = 0.088 µM
K_i = 4.2 µM
K_i/K_m = 48
1/dpm x 10^{-4}
1/dGTP (μM^{-1})
D
(L/D)-(-/+)-G-α-CNP inhibition of HCMV DNA polymerase
◆ 27 µM ▲ 13.5 µM ■ 6.7 µM ○ Control
K_m = 0.71 µM
K_i = 8.6 µM
K_i/K_m = 12
1/dpm x 10^{-4}
1/dGTP (μM^{-1})

Fig. 2

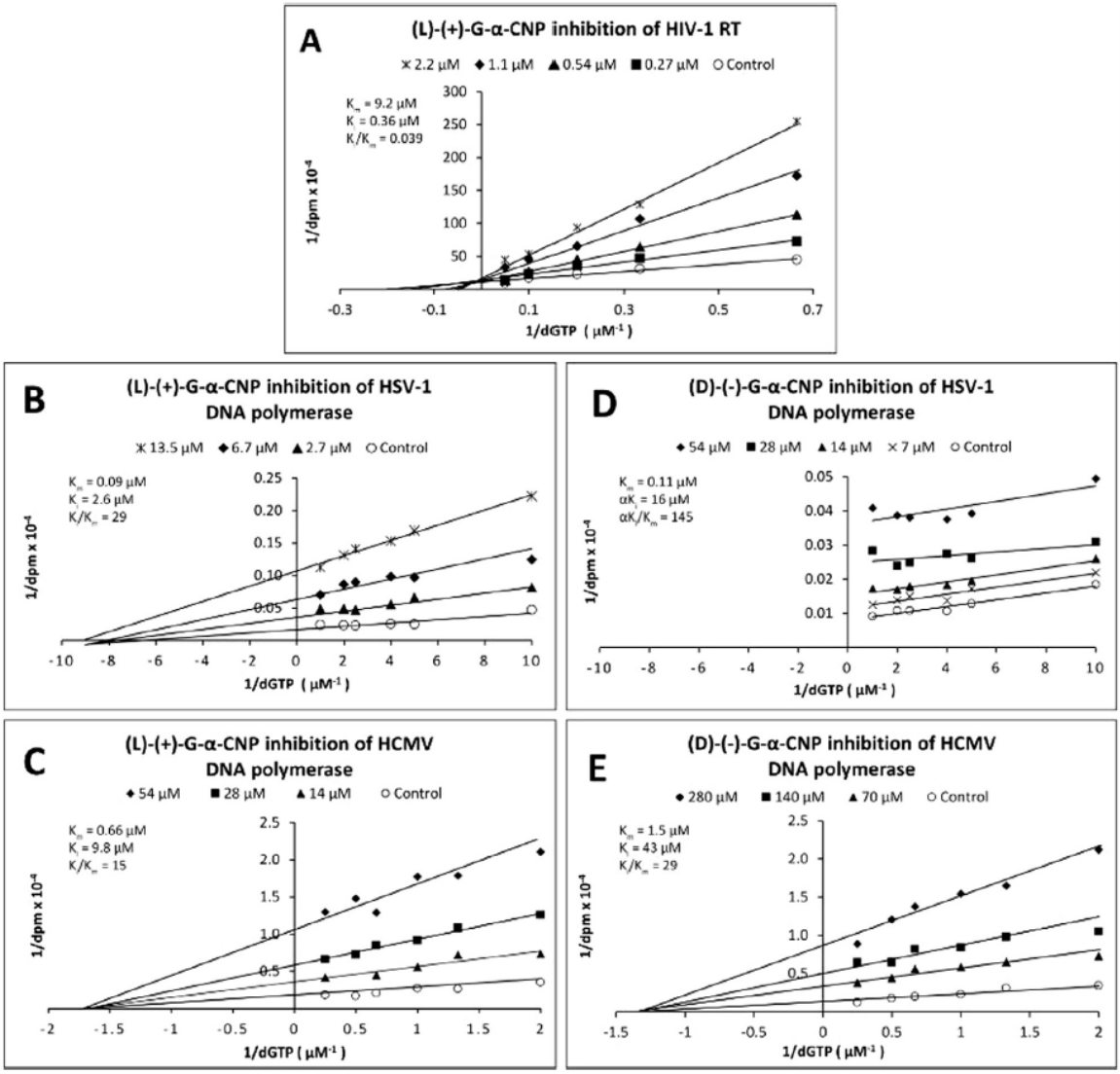
A
(L)-(+)-G-α-CNP inhibition of HIV-1 RT
2.2 μM
1.1 μM
0.54 μM
0.27 μM
Control
K_m = 9.2 μM
K_i = 0.36 μM
K_i/K_m = 0.039
1/dpm x 10^{-4}
1/dGTP (μM^{-1})
B
(L)-(+)-G-α-CNP inhibition of HSV-1 DNA polymerase
13.5 μM
6.7 μM
2.7 μM
Control
K_m = 0.09 μM
K_i = 2.6 μM
K_i/K_m = 29
1/dpm x 10^{-4}
1/dGTP (μM^{-1})
D
(D)-(-)-G-α-CNP inhibition of HSV-1 DNA polymerase
54 μM
28 μM
14 μM
7 μM
Control
K_m = 0.11 μM
αK_i = 16 μM
$\alpha K_i/K_m$ = 145
1/dpm x 10^{-4}
1/dGTP (μM^{-1})
C
(L)-(+)-G-α-CNP inhibition of HCMV DNA polymerase
54 μM
28 μM
14 μM
Control
K_m = 0.66 μM
K_i = 9.8 μM
K_i/K_m = 15
1/dpm x 10^{-4}
1/dGTP (μM^{-1})
E
(D)-(-)-G-α-CNP inhibition of HCMV DNA polymerase
280 μM
140 μM
70 μM
Control
K_m = 1.5 μM
K_i = 43 μM
K_i/K_m = 29
1/dpm x 10^{-4}
1/dGTP (μM^{-1})

Fig. 3

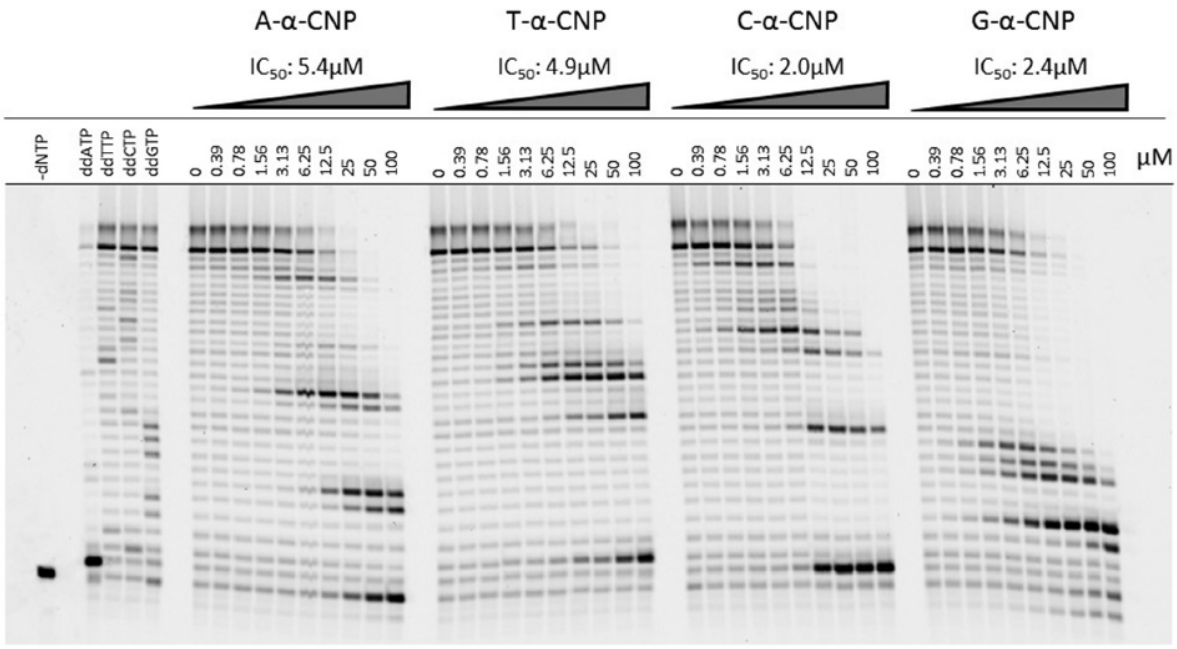
A-α-CNP
IC50: 5.4μM
T-α-CNP
IC50: 4.9μM
C-α-CNP
IC50: 2.0μM
G-α-CNP
IC50: 2.4μM
-dNTP
ddATP
ddTTP
ddCTP
ddGTP
0
0.39
0.78
1.56
3.13
6.25
12.5
25
50
100
μM

Fig. 4

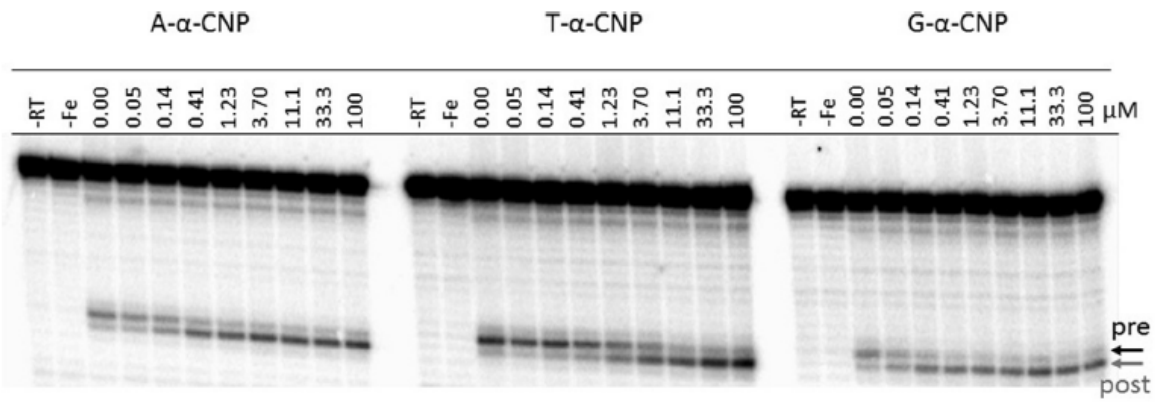
A-α-CNP
T-α-CNP
G-α-CNP
-RT
-Fe
0.00
0.05
0.14
0.41
1.23
3.70
11.1
33.3
100
μM
pre
post

Fig. 5

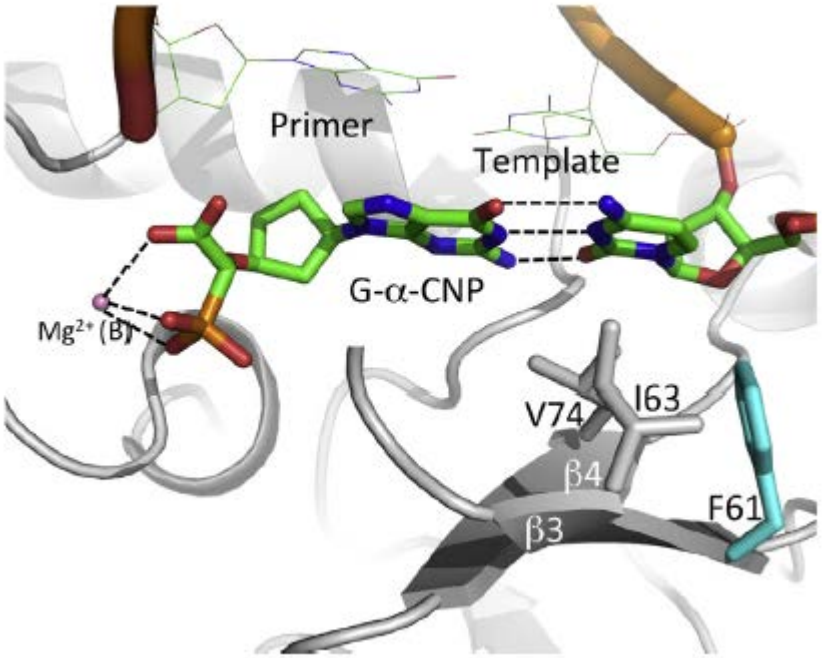

Fig. 6